Electronic Supplementary Material (ESI) for CrystEngComm.

Supporting Information

Piezochromic Luminescent Tuning of Donor-Acceptor Cocrystals to Grinding and Isotropic Compression

Shuai Wang, Wenxin Xiang, Chen Pan, Jinqiu Chen, Wenju Li, Jing Zhang*, Jianfeng Zhao* and Guangfeng Liu*

*__Jing Zhang__ - State Key Laboratory of Organic Electronics and Information Displays & Institute of Advanced Materials (IAM), Nanjing University of Posts & Telecommunications, 9 Wenyuan Road, Nanjing 210023, China;
E-mail: iamjingzhang@njupt.edu.cn.
***Jianfeng Zhao** - Key Laboratory of Flexible Electronics (KLOFE) & Institute of Advanced Materials (IAM), Jiangsu National Synergetic Innovation Center for Advanced Materials (SICAM), Nanjing Tech University (NanjingTech), 30 South Puzhu Road, Nanjing 211816, China;
E-mail: iamjfzhao@njtech.edu.cn.
*__Guangfeng Liu__ - Department of Chemistry, Uniwersitcé Libre de Bruxelles, Avenue F. D. Roosevelt 50, 1050, Brussels, Belgium;
E-mail: gliu@ulb.ac.be.
Jiangsu Key Laboratory of Advanced Catalytic Materials & Technology, School of Petrochemical Engineering, Changzhou University, Changzhou 213164, China;

Table of Contents

Experimental Procedures

Materials. BNF and TCNB were purchased from Bide Pharmatech Ltd. and Luminescence Technology Corp, respectively. Both of them were used directly as received without further purification. All solvents were HPLC grade.

Cocrystals Growth and Structural Analysis. *α*- and *β*-BNF-TCNB complexes were prepared from solvent evaporation from dichloroethane and tetrahydrofuran solution, respectively. First, we dissolved the BNF and TCNQ mixtures with a molar ratio of 1:1 in dichloroethane or tetrahydrofuran to get the blend solution with a concentration of ~2.64 mg/mL. After heating at about 80 °C for about 1 hour to ensure complete dissolution, the mixed solution was left in the table until the complete solvent evaporation for several days, and then crystal products were found at the bottom of the bottle. Subsequently, the ribbon cocrystals were washed from the vial with petroleum ether and dried in air. The Bruker smart-1000-CCD diffractometer with graphite-monochromatic Mo *K*α radiation (λ = 0.71073 Å) was used to measure the crystal structure of *α*-BNF-TCNB. The Bruker smart-1000-CCD diffractometer with graphite-monochromatic Cu *K*α radiation (λ = 1.541 Å) was used to measure the crystal structure of *β*-BNF-TCNB. The structures were resolved by the direct method and refined by the full-matrix least-squares method on F^2 using the SHELXL-97 program.

Piezochromic Luminescent Tests of *α*-crystal. The grinding experiment: 2-3 milligrams of crystals was put in a mortar and then ground by the pestle for several minutes. For the isotropic compression test, 6-10 milligram crystals were compactly put in the space of lab tablet press for a circular slice, and then gradual and different pressure was applied onto the machine.

Measurements. The optical and fluorescent images of the samples were characterized by fluorescence microscope (BX53, Leica), PXRD was measured on a D/max2500 with Cu *K*α source (κ = 1.541 Å). The DSC analysis were recorded on DSC2A-01130 at a temperature ramp of 10 °C/min under N_2. The calculations of the molecular energy levels were calculated by DFT at the B3LYP/6-31G level. The calculation of charge-transfer degree was performed with the Mulliken population analysis.

Calculation method. The crystal growth morphology of α-BNF-TCNB was predicted using the software CCDC-Mercury 2020.3.0 based on the Bravais–Friedel–Donnay–Harker (BFDH) method.[1-3] Energy frameworks[4, 5] offer a powerful tool to visualize the molecular interaction energy in crystal structures, which are calculated and mapped using the software *CrystalExplorer* 17.[6] Energy frameworks energies between molecular pairs are represented as cylinders joining the centroids of pairs of molecules, with the cylinder radius proportional to the magnitude of the interaction energy. Frameworks can be constructed for total energy E_{tot} (blue). An overall scale factor is used to expand or contract the framework cylinders, under the same scale factor the energy frameworks can be directly comparable. The energy of interaction between molecules is commonly expressed in terms of four key components: electrostatic (E_{ele}), polarization (E_{pol}), dispersion (E_{dis}), and exchange-repulsion (E_{rep}), given by

$$E_{tot} = k_{ele}E_{ele} + k_{pol}E_{pol} + k_{dis}E_{dis} + k_{rep}E_{rep}$$

Where, *k* is the scale factor, accurate values of these component are obtained based on models (i.e., HF/3-21G, MP2/6-31G(d,p) and B3LYP/6-31G(d,p)).

Results and Discussion

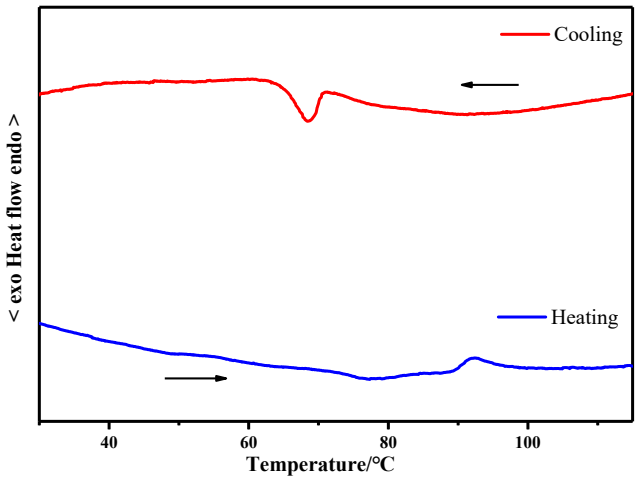

Fig S1. DSC curve of the *α*-cocrystal sample with rate of 10 °C/min in a heating–cooling cycle.

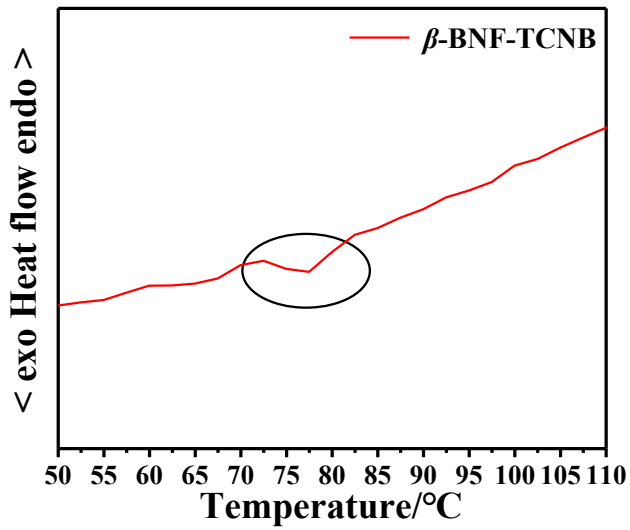

Fig S2. DSC curve of the *β*-cocrystal sample with rate of 10 °C/min in the cooling cycle.

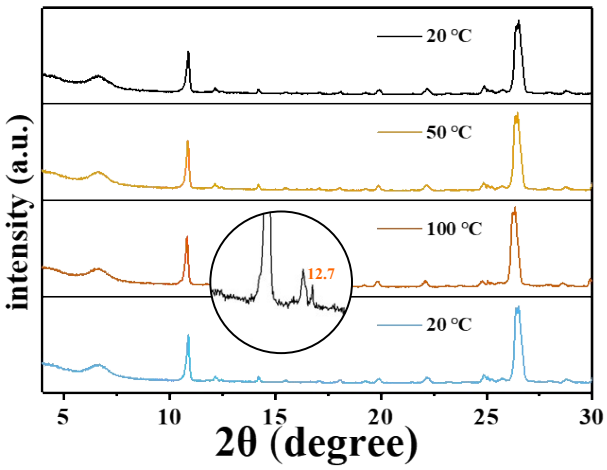

Fig S3. Variable-temperature PXRD results of *α*-BNF-TCNB cocrystals.

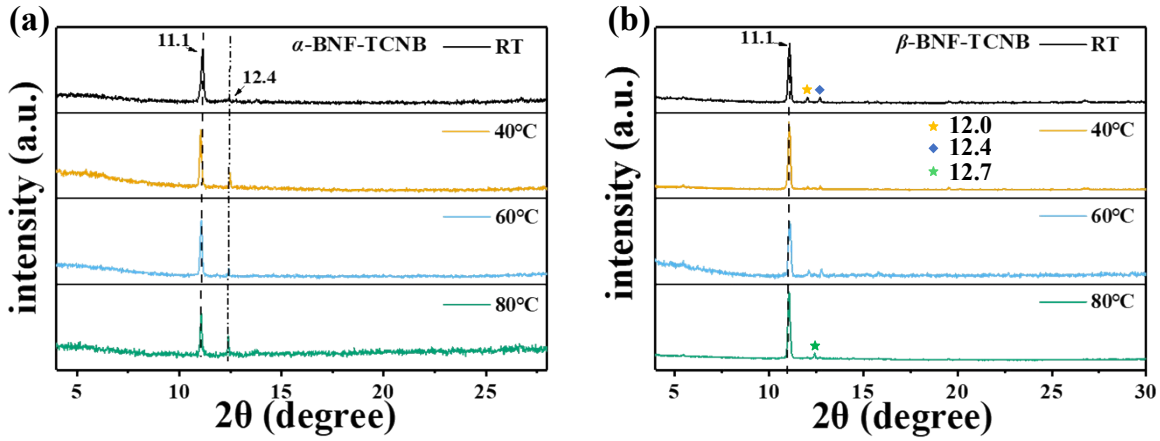

Fig S4. PXRD results of annealed cocrystals of *α*-BNF-TCNB and *β*-BNF-TCNB at different temperatures. The samples were tested at room temperature. The PXRD of several cocrystals after annealing demonstrated a reversible phase transition from *α*-crystals, but annealed *β*-crystal would turn to *α*-crystal without the recovery, hence the results demonstrated the *β*-form was metastable at room temperature

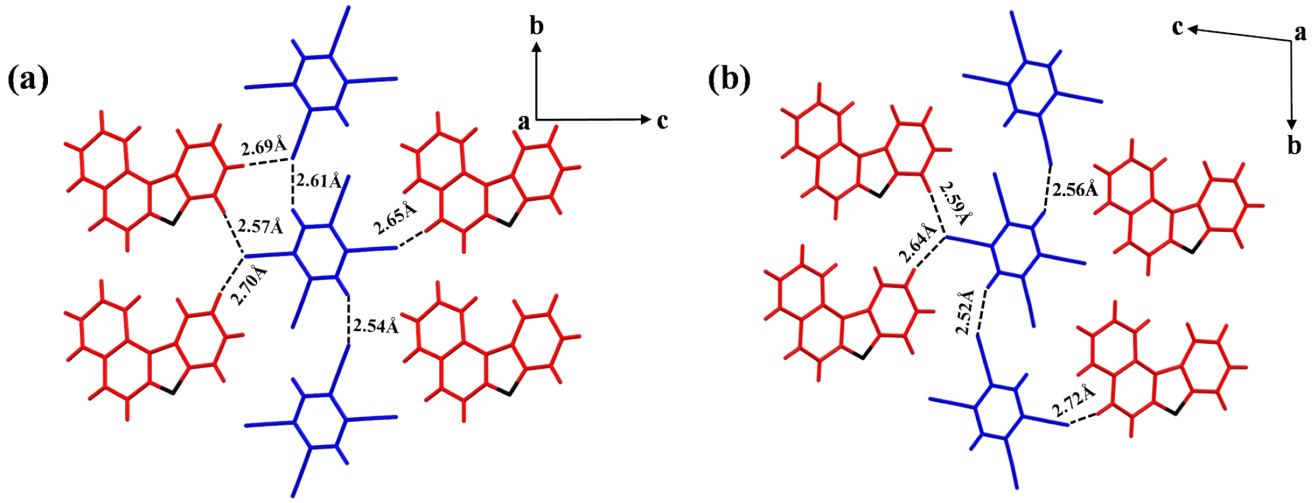

Fig S5. (a) C-H···N intermolecular interactions of *α*-crystal and (b) *β*-crystal.

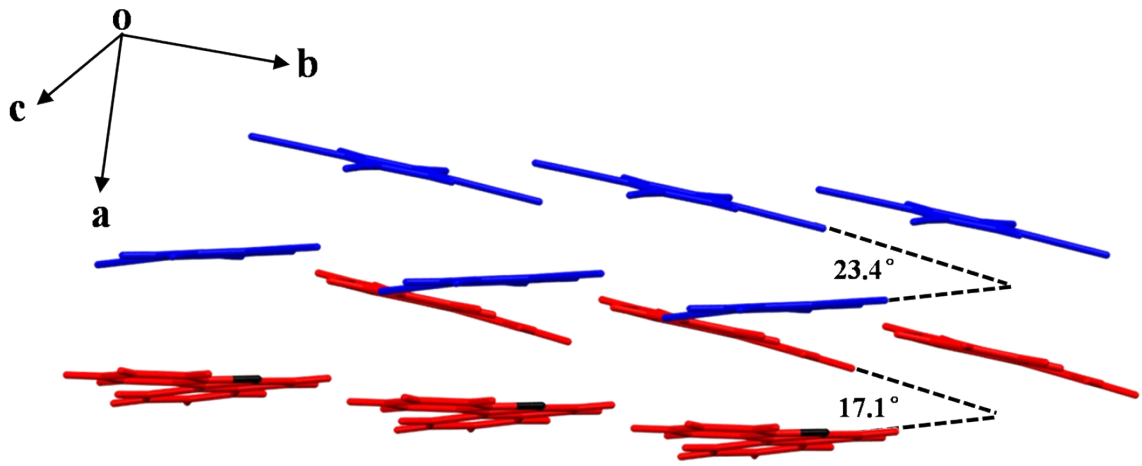

Fig S6. The slipping angles of TCNB molecules and BNF cores in alternated columns

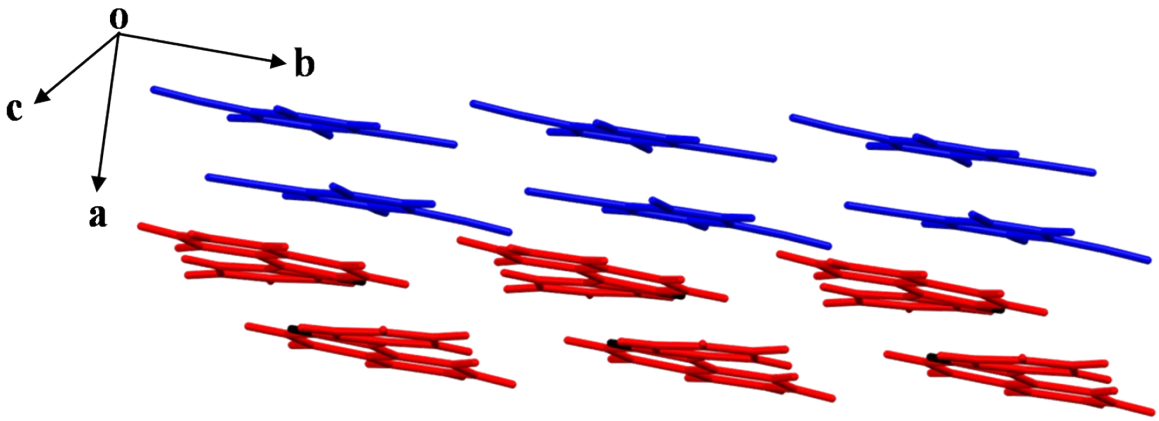

Fig S7. The slipping angle disappearance in *β*-cocrystal.

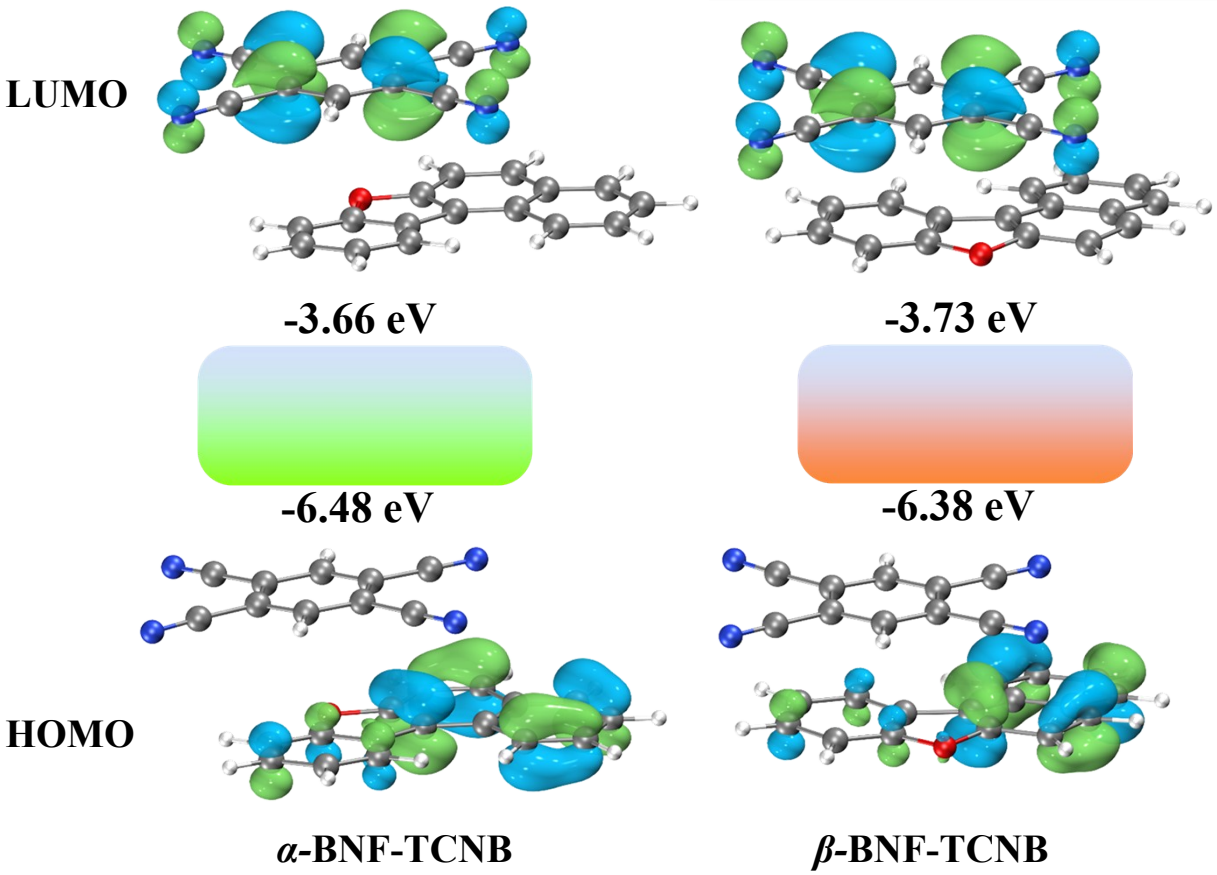

Fig S8. The HOMO and LUMO energy level diagram of two crystal forms.

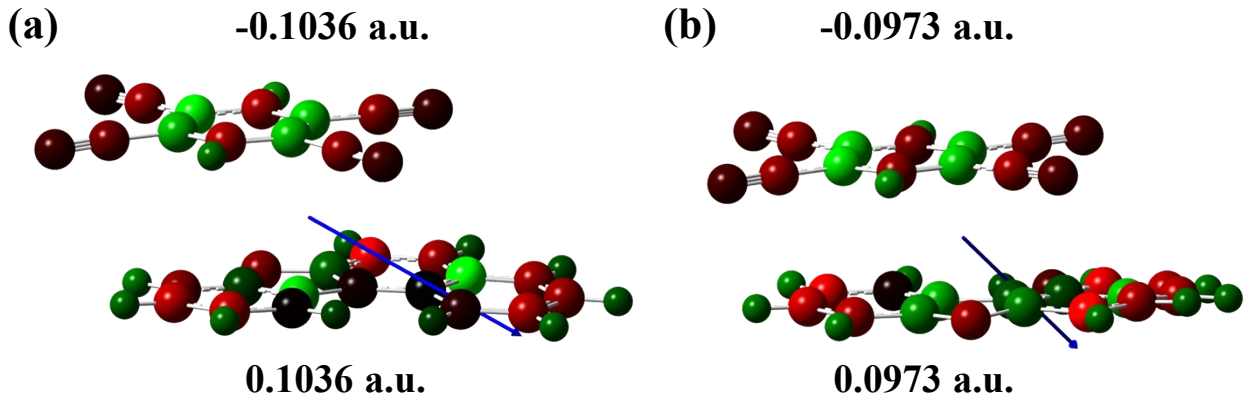

Fig S9. The charge-transfer degree of (a) *α*-crystal and (b) *β*-crystal.

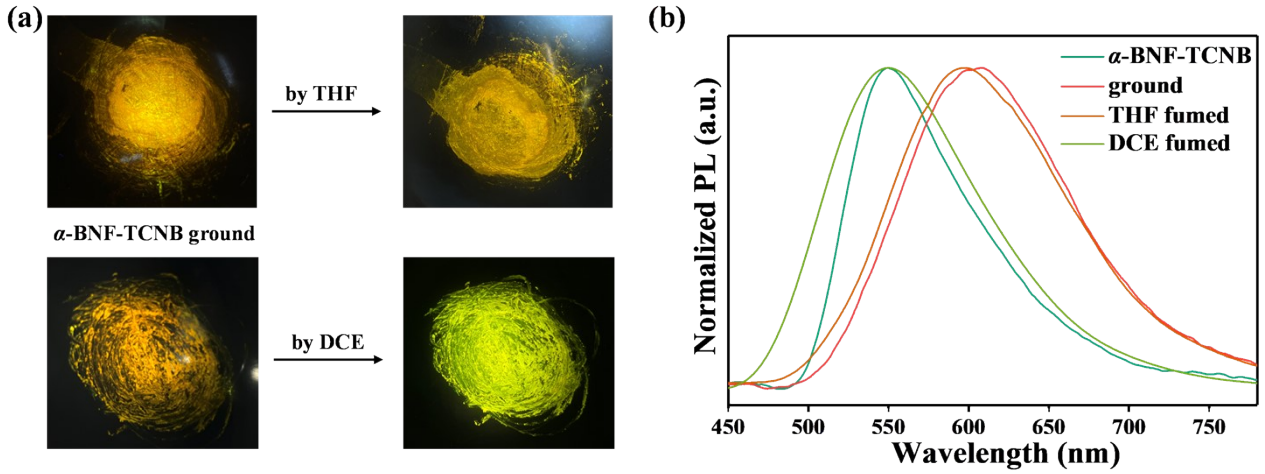

Fig S10. (a)The fluorescent images of *α*-BNF-TCNB ground and fumed by THF and DCE under illumination with UV light (365 nm), (b) the corresponding PL spectra.

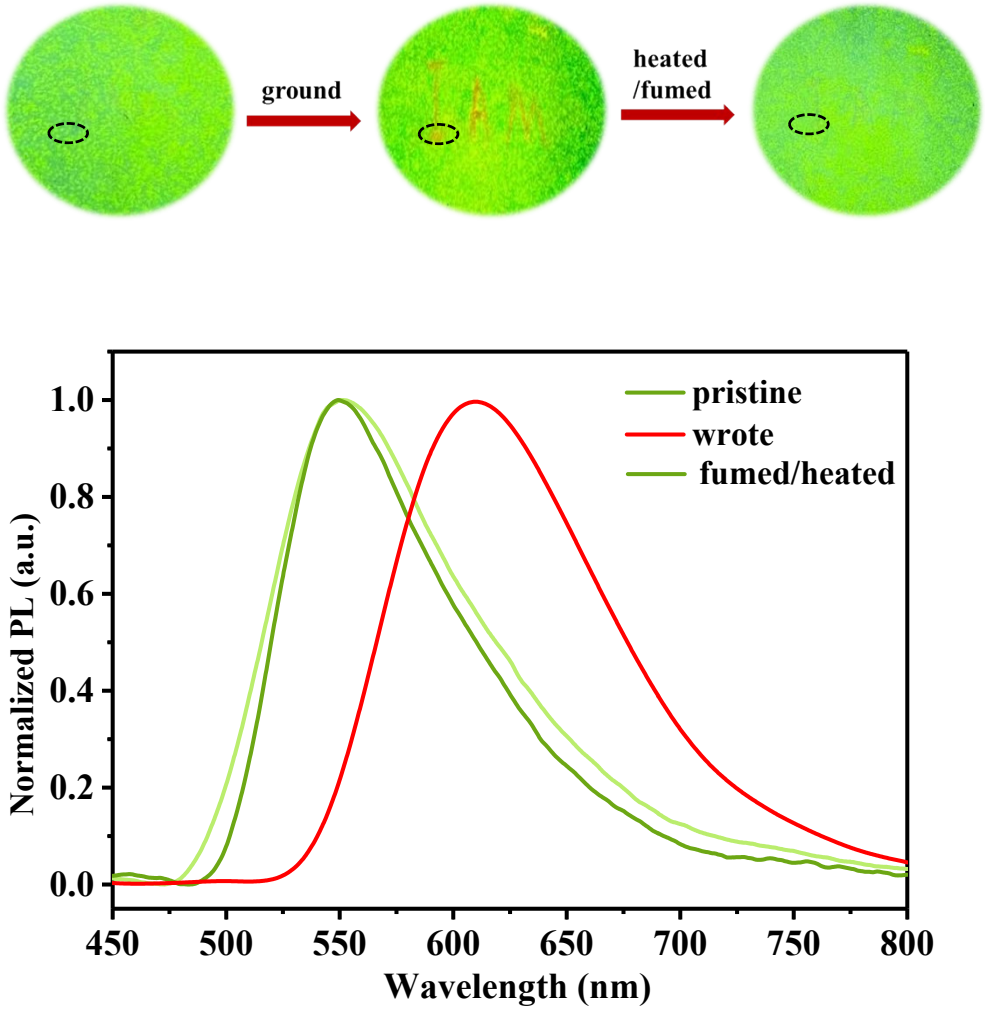

Fig S11. Writing and erasing an 'IAM' letter on the cocrystal coated weighing paper, and the corresponding PL spectra change.

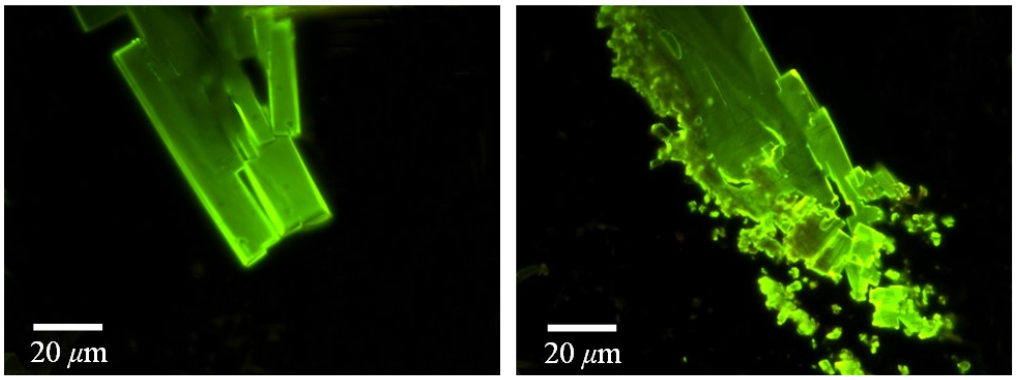

Fig S12. Press vertically on one individual crystal which will damage the crystal, but no color change was found (no crystal transition).

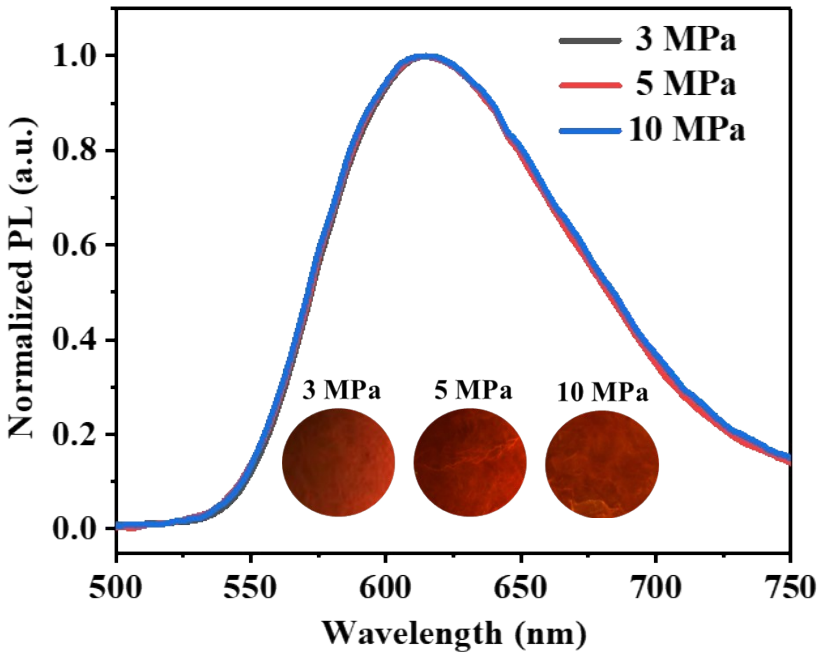

Fig S13. Fluorescence images of *α*-crystal pellet under compression pressure larger than 3 MPa.

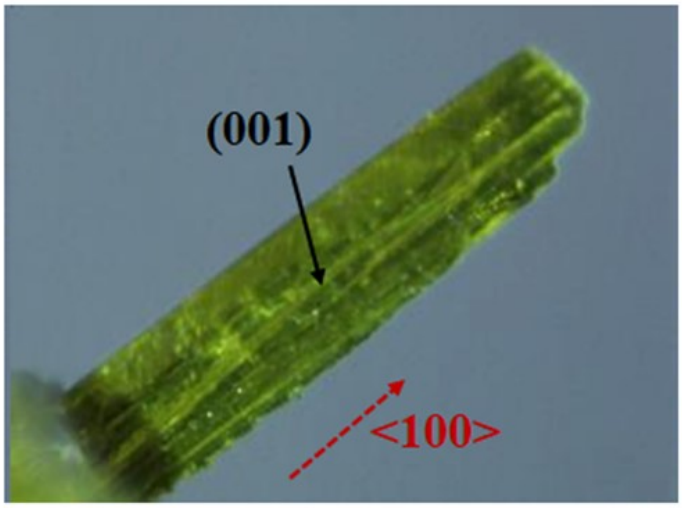

Fig S14. The face indexing of the crystal α-BNF-TCNB.

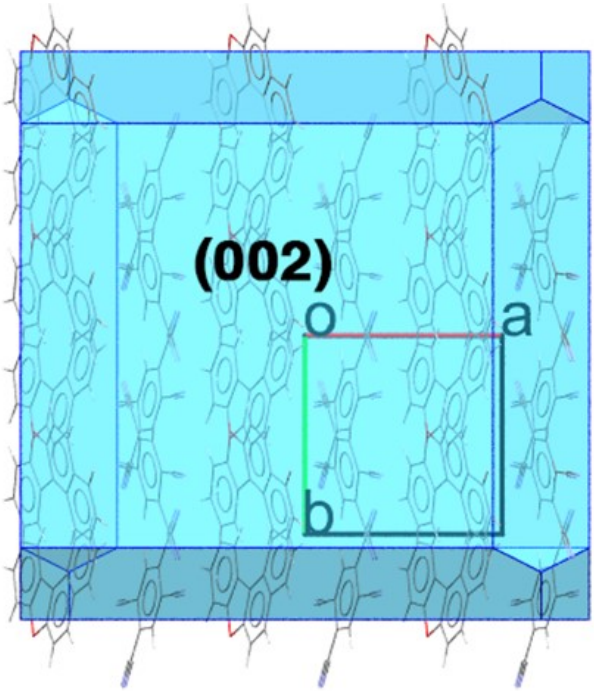

Fig S15. The calculated morphology of the crystal α-BNF-TCNB.

Table S1. Crystal data and structure refinements for *α*- and *β*-DNF-TCNB cocrystals.

	α-BNF-TCNB	*β*-BNF-TCNB
Formula	$C_{26}H_{12}N_4O$	$C_{26}H_{12}N_4O$
Formula weight	396.40	396.40
Temperature (K)	193	193
Wavelength (Å)	0.71073	1.54178
Crystal system	Monoclinic	Triclinic
space group	*P*1c1	*P* -1
Unit cell dimensions		
a (Å)	7.9325(3)	7.9376(8)
b (Å)	7.8534(4)	7.9412(8)
c (Å)	15.8599(8)	15.8417(18)
α (°)	90	93.490(9)
β (°)	99.753(2)	100.212(8)
γ (°)	90	92.313(8)
Volume (Å^3)	973.75(8)	979.59(18)
Z	2	2
Absorption coefficient (mm^{-1})	0.086	0.682
F(000)	408.0	408.0
Crystal size (mm)	0.16 × 0.15 × 0.12	0.15 × 0.12 × 0.1
θ range (°)	2.594 to 27.487	2.841 to 70.916
Limiting indices	-10 ≤ *h* ≤ 10	-9 ≤ *h* ≤ 9
	-10 ≤ *k* ≤ 8	-9 ≤ *k* ≤ 9
	-18 ≤ *l* ≤ 20	-19 ≤ *l* ≤ 19
Reflections collected	4474	3788
R(int)	0.0740	0.0105
Absorption correction	Semi-empirical from equivalents	Semi-empirical from equivalents
Refinement method	Full-matrix least-squares on F^2	Full-matrix least-squares on F^2
R [*I* > 2sigma(*I*)]	R_1 = 0.0740	R_1 = 0.1050
	wR_2 = 0.2023	wR_2 = 0.2910
R (all data)	R_1 = 0.0853	R_1 = 0.1449
	wR_2 = 0.2152	wR_2 = 0.3339
CCDC NO.	2238828	2238829

References:
1. A. Bravais, Etudes Cristallographiques, Gauthier-Villars, 1866.
2. G. Friede and Crystal Morphologies, Bull. Soc. Fr. Mineral.,1907, 30, 326–455.
3. J. D. H. Donnay and D. Harker, A new law of crystal morphology extending the law of Bravais, Am. Mineral., 1937, 22, 446–467.
4. M. J. Turner, S. P. Thomas, M. W. Shi, D. Jayatilaka and M. A. Spackman, Chem. Commun., 2015, 51, 3735–3738.
5. M. J.Turner, S. Grabowsky, D. Jayatilaka and M. A. Spackman, J. Phys. Chem. Lett., 2014, 5, 4249–4255.
6. M. J. Turner, J. J. McKinnon, S. K. Wolff, D. J. Grimwood, P. R. Spackman, D. Jayatilaka and M. A. Spackman, CrystalExplorer17 (2017).